Arabian Journal for Science and Engineering (2024) 49:7783–7794
https://doi.org/10.1007/s13369-020-04760-8

RESEARCH ARTICLE-CHEMICAL ENGINEERING

Biosynthesized Silver Nanoparticles for Colorimetric Detection of Fe^{3+} Ions

Deniz Uzunoğlu[1] · Memduha Ergüt[1] · Cemile Gamze Kodaman[1] · Ayla Özer[1]

Received: 3 October 2019 / Accepted: 1 July 2020 / Published online: 17 August 2020

Abstract
In this study, the biosynthesis and characterization of silver nanoparticles (AgNPs) from orchid tree (*Bauhinia variegata*) leaf extract were firstly carried out, and then, the usability of AgNPs as a colorimetric sensor for detection of Fe^{3+} ions in aqueous solutions was evaluated. The characterization studies showed that the synthesized particles were determined to be AgNPs in nanoscale and face-centered cubic structure. Besides, the total phenolic content of *B. variegata* extract was determined to be 1.826 ± 2.1 mg gallic acid equivalents/g dry leaf. Also, the biosynthesized AgNPs showed a strong surface plasmon resonance (λ_{SPR}) around 430 nm and λ_{SPR} intensity decreased with the increasing in Fe^{3+} concentration in aqueous solution. Based on the linear relationship between the change of λ_{SPR} intensity and Fe^{3+} ion concentration, AgNPs can be used for the sensitive and selective detection of Fe^{3+} ions in aqueous solutions with a linear range of 6-100 µM and a detection limit of 2.08×10^{-6} M.

Keywords *Bauhinia variegata* leaf extract · Biosynthesis · Colorimetric sensor · Detection of Fe^{3+} ions · Silver nanoparticles

1 Introduction

There is a global threat due to heavy metal pollution since the inception of the industrial revolution. Heavy metals like Zn, Fe, Cu, Pb, Ni, Cd, Hg, etc., are widely processed in many industries like paper industries, pesticides, tanneries, metal plating industries, mining operations, etc. The wastewater discharge from these industries causes to various environmental problems due to its toxic nature. They are also non-biodegradable and enduring components; therefore, serious health and environmental hazards have been stemmed from the heavy metals in the receiving effluents at even low concentrations [1]. For these reasons, it is crucial to detect and monitor them in both aqueous environmental and biological samples with high sensitivity and selectivity. There are various analytical techniques such as atomic absorption spectrometry [2], inductively coupled plasma mass spectrometry [3], inductively coupled plasma emission spectrometry [4], high-performance liquid chromatography [5], anodic stripping voltammetry [6], adsorptive stripping voltammetry [7], flow injection chemiluminescence manifold [8], and UV–visible spectrophotometer [9] for the detection of metal ions. However, these methods usually require sophisticated equipments, technical expertise, and tedious sample preparation steps. Therefore, it is thought that these techniques are not economical and user-friendly. In order to overcome these disadvantages, the colorimetric sensors have been developed for the detection of metal ions in aqueous solutions. Nowadays, especially metallic nanoparticle-based sensors have been widely used for colorimetric detection of metal ions [10–13] due to their strong surface plasmon resonance (SPR), stable dispersion, bio-compatibility, and controllable physical/chemical properties. The principle of colorimetric detection with nanoparticle-based sensors is the same as the spectrophotometric method. However, the ordinary spectrophotometric methods required costly and time-consuming steps such as flow injection, synthesis of complexing reagents, and sample preparation [9, 11–17]. When these studies were examined in detail, it could be easily seen that these methods required costly and time-consuming steps such as flow injection, synthesis of complexing reagents, and sample preparation although the detection limits were low. Also, the detection time is mostly too long compared

✉ Deniz Uzunoğlu
denizuzunoglu4@gmail.com

[1] Department of Chemical Engineering, Faculty of Engineering, Mersin University, Mersin 33343, Turkey

to the sensor processes because the detection with a sensor is an in situ method that allows real-time monitoring (quick response). Therefore, it is an effective alternative to detect metal ions with metallic nanoparticle-based sensors [18–20]. Among the metallic nanoparticles, it is well known that silver nanoparticles (AgNPs) have the strongest SPR; for this reason, most of SPR-related fundamental investigations and sensing applications have focused on AgNPs [18]. However, in the literature, it has been quite common to use the functionalized metallic nanoparticles for the colorimetric detection of metal ions [21–25]. The functionalization is both costly and time-consuming process; therefore, it is important to study with environmental-friendly, non-functionalized, and so low-cost nanoparticle-based sensor.

The electrochemical method [26, 27], reverse micelles/microemulsion method [28, 29], hydrothermal synthesis [30, 31], sonochemical method [32, 33], chemical precipitation [34, 35], chemical reduction [36], and sol–gel method [37] have been conventionally used for the synthesis of metallic nanoparticles. However, there are some disadvantages of these methods such as the use of hazardous chemicals and toxic materials, low conversion, difficult, costly and time-consuming purification requirements, and high energy demand. In this regard, nowadays, biosynthesis method, which uses the biological reductant agents such as microorganisms, enzymes, and plants, has attracted much attention. The principle of biosynthesis of nanoparticles depends on the reduction of metal ions in the metal salt solutions to the nanoparticles with the aid of biological reductant agents. Among these biological reductant agents, there are many advantages of plants such as availability, no need to sterilization, easy, and safe to be processed of plants. On the other hand, using plants in metallic nanoparticle biosynthesis provides to convert unused resources into economic value [38]. In this regard, the biosynthesis method using plants has been frequently preferred for the synthesis of metallic nanoparticles [39–41]. For these reasons, in this study, AgNPs were biosynthesized with a green, simple, one-pot, low-cost, and stabilizer-free method for the detection of Fe^{3+} ions in aqueous solutions. It is the first time both to evaluate *B. variegata* leaf extract in the biosynthesis of AgNPs and to utilize these AgNPs in the colorimetric detection of Fe^{3+}. Therefore, it can be said that this work has a novelty in terms of these subjects, which will provide contributions to the related literature.

2 Materials and Methods

2.1 Materials

$AgNO_3$ (Merck, ≥ 99.0%), Na_2CO_3 (Merck, ≥ 99.9%), $AgNO_3$ (Merck, ≥ 99.0%), $MgSO_4$ (Merck, ≥ 98.0%), $BaCl_2$ (Merck, ≥ 99.995%), $NiSO_4*6H_2O$ (Merck, ≥ 99.0%), $MnSO_4*H_2O$ (Merck, ≥ 98.0%), $Cu(NO_3)_2*3H_2O$ (Merck, ≥ 99.5%), $ZnSO_4*7H_2O$ (Merck, ≥ 99.5%), $FeCl_3*6H_2O$ (Merck, ≥ 99.0%), $Cd(NO_3)_2*4H_2O$ (Sigma-Aldrich, ≥ 98.0%), Folin–Ciocalteu's phenol reagent (2 N, Merck, ≥ 99%), gallic acid (Sigma-Aldrich, ≥ 99%) were used in the experiments. All of them were of analytical grade, and they were used without further purification.

2.2 Biosynthesis and Characterization of AgNPs

Firstly, AgNPs were synthesized via the biosynthesis method by using the aqueous extract of Orchid tree (*Bauhinia variegata*) leaves. For this purpose, *B. variegata* leaves were collected from Çiftlikköy Campus of Mersin University in Turkey and they were washed with firstly tap water and then distilled water; after that, they were dried in an oven at 50 °C for 24 h. Then, 5.0 g of the purified and dried leaves were boiled in 600 mL of distilled water. The total phenolic content (TPC) of the aqueous extract of *B. variegata*, which is important for the reduction of $AgNO_3$ to AgNPs, was designated via Folin–Ciocalteu colorimetric method. For this purpose, 200 µL Folin–Ciocalteu reagent and 2.8 mL of distilled water were put into 400 µL of the aqueous extract and the solution was vortexed. After 5 min, 600 µL of 20% Na_2CO_3 solution was added to the as-prepared mixture and the solution was vortexed again. Subsequently, the solution was incubated for 2.0 h at room temperature in the dark. At the end of the incubation process, the blue solution was obtained and the absorbance of this solution was measured at 765 nm against the blank by UV–Vis spectrophotometer (Specord 210 Plus, Analytik Jena, Germany). TPC was stated as gallic acid equivalent (GAE) (mg of gallic acid/g dry matter), using the standard curve prepared at different concentrations (100–700 mg/L) of gallic acid [42].

As-prepared aqueous leaf extract was then used as a reducing agent in the biosynthesis of AgNPs. In the biosynthesis of AgNPs, 5.0 mL of the aqueous leaf extract was added to 100 mL of 10^{-3} M $AgNO_3$ solution, and then, the mixture was stirred magnetically at room temperature for 1.0 h. After that, the resulting mixture was centrifuged at 8000 rpm and the precipitated AgNPs were washed with distilled water and dried at 110 °C in the oven for 24 h [43]. Finally, 0.015 g of the dried AgNPs was dispersed in 100 mL of distilled water for the colorimetric detection studies. The dried AgNPs were used for characterization studies such as X-ray Diffractometer (XRD-Philips XPert, Netherlands), zetasizer (Malvern, UK) using Dynamic Light Scattering (DLS) technique, and Fourier-Transform Infrared Spectrometer (FT-IR-PerkinElmer, Shelton).

2.3 Chemical Synthesis of AgNPs

AgNPs were synthesized via the chemical reduction method using $NaBH_4$ reductant agent. For this purpose, 25 mL of 10^{-3} M $AgNO_3$ solution was dropped by a syringe pump with a flow rate of 1.0 mL/min to the freshly prepared and ice-cold 75 mL of 2×10^{-3} M $NaBH_4$ solution in an Erlenmeyer that was put into an ice bath. The mixture was stirred magnetically for 5.0 h, and the color of the solution began to turn light yellow as $AgNO_3$ solution was added. Finally, the stable dark yellow solution was obtained after the solution was left at the room conditions for 24 h. The as-synthesized AgNPs were separated with a centrifuge at 14,000 rev.min^{-1} for 10 min, washed with distilled water, and then dried in an oven at 60 °C for 12 h. The dried AgNPs were dissolved in distilled water that its concentration was to be 0.15 g/L. The formation of chemically synthesized AgNPs was analyzed with UV spectrophotometer [44].

2.4 Colorimetric Detection

The colorimetric detection studies of the different species such as Na^+, K^+, Mg^{2+}, Ba^{2+}, Ni^{2+}, Mn^{2+}, Cu^{2+}, Zn^{2+}, Cd^{2+}, and Fe^{3+} with the biosynthesized AgNPs were carried out by a series of experiments. 1.0 mL of 1000 µM metal ion solution was added to the mixture containing 2.0 mL of 0.15 g/L AgNPs solution and 1.0 mL of the distilled water. Approximately 5.0 min later, the absorbance value of the prepared solution was recorded at 430 nm by UV–Vis spectrophotometer and their spectra were scanned at a wavelength range of 300–700 nm. Experimental and analysis methods were repeated for the other metal ions. The maximum decrease in the SPR of AgNPs and disappearance of color was observed only in the presence of Fe^{3+}. Thus, different concentrations of Fe^{3+} (1–100 µM) were used to determine the linear detectable range and limit of detection by means of decreasing in the λ_{SPR} intensity of AgNPs [18].

3 Results and Discussion

The results of the nanoparticle synthesis, characterization, and the colorimetric detection of the metal ions with the silver nanoparticles (AgNPs) were given in the following subsections.

3.1 Characterization of AgNPs

The formation of AgNPs was firstly determined by visual observation of the color of AgNPs solution, and then, the UV–Vis spectra of the solutions were performed against distilled water with 1.0 mm optical path length quartz cuvette. Figure 1 shows the UV–Vis spectrums of $AgNO_3$, *B. variegata* leaf extract, and AgNPs. As shown in Fig. 1, the bond at 330 nm was observed for *B. variegata* leaf extract, which could be attributed to $\pi\rightarrow\pi^*$ transitions, being assigned to the presence of polyphenolics as the reductant and stabilizer agent employed for the biosynthesis of AgNPs. In the biosynthesis method, *B. variegata* leaf extract was added to $AgNO_3$ solution, leading to the reduction of Ag^{1+} ions to Ag^0 (AgNPs) and visual color change from yellow to brown. This color change was due to the excitation of surface plasmon resonance (SPR) of AgNPs. The strong SPR band for AgNPs was noticed around 430 nm. This band was observed in the ideal wavelength range provided for AgNPs solution [45]. Furthermore, the studies in the literature have suggested that the shape of the particles giving SPR peak in the range of 410–500 nm is spherical, while SPR bands of pentagons and triangular shapes mostly formed in the range of 500-700 nm. This observation suggested that in this study, AgNPs were synthesized in spherical forms [46].

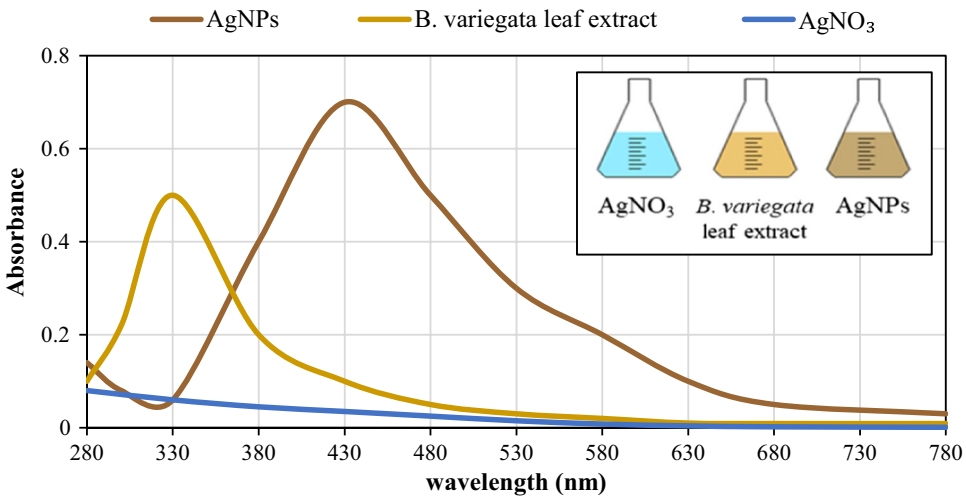

Fig. 1 UV–Vis spectrums of $AgNO_3$, *B. variegata* leaf extract, and AgNPs

The spectrum scan of the chemically synthesized AgNPs was recorded in the wavelength range of 250–1000 cm^{-1}, and the recorded spectrum scan is given in Fig. 2. Accordingly, the surface plasmon resonance (SPR) produced a peak at 400 nm, which is the characteristic peak of AgNPs. The obtained stable dark yellow color and the SPR at 400 nm confirmed the formation of silver nanoparticles.

FT-IR analysis was carried out in order to determine the functional groups of AgNPs, and the FT-IR spectrum is presented in Fig. 3. Accordingly, the peaks corresponding to O–H group in polyphenols (3250 cm^{-1}), =C–H alkenes (2983 cm^{-1}), –COOH carbonyl group (1572 cm^{-1}), –C–H alkane (1309 cm^{-1}), C–N stretch aliphatic amines (1100 cm^{-1}), C–N amines (1095 cm^{-1}), C–C bending (660 cm^{-1}) were determined from FT-IR spectra of AgNPs [47, 48].

The presence of polyphenolics was observed in UV–Vis and FT-IR spectra. So, TPC of *B. variegata* extract was determined by Folin–Ciocalteu colorimetric method. Accordingly, TPC value was determined to be 1.826 ± 2.1 mg GAE/g dry leaf. Consequently, the obtained SPR value of *B. variegata* extract, FT-IR peak of AgNPs related to polyphenols, and the calculated phenolic content of *B. variegata* extract confirmed that the phenolic substances in the aqueous leaf extract played important roles in the reduction of Ag^{1+} ($AgNO_3$) into Ag^0 (AgNPs).

The crystal phase of AgNPs was determined by XRD analysis method (Fig. 4). The peaks at 2θ angles of 38.10°, 44.28°, 64.41°, and 77.36° corresponded to the crystal planes of [1 1 1], [2 0 0], [2 2 0], and [3 1 1]. This typical powder XRD pattern indicated that AgNPs had the face-centered cubic structure [49]. However, there were some unassigned peaks indicating the crystallization of bio-organic phase (as obtained in FT-IR spectra) on the AgNPs surface due to the aqueous leaf extract [50].

SEM analysis was conducted for the evaluation of the AgNPs morphology, and the obtained SEM image is presented in Fig. 5. As predicted in UV–Vis spectra of AgNPs, nearly spherical-like nanoparticles were synthesized via the biosynthesis method.

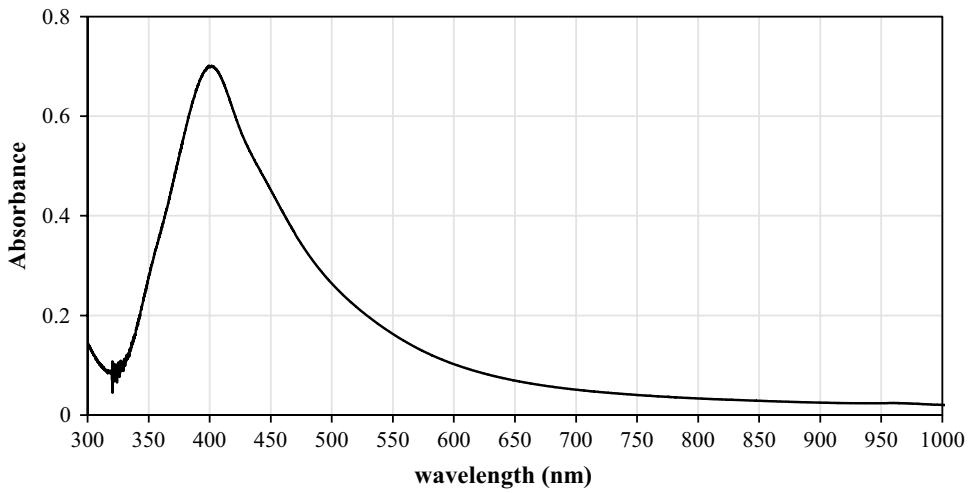

Fig. 2 UV–Vis spectrum of the chemically synthesized AgNPs

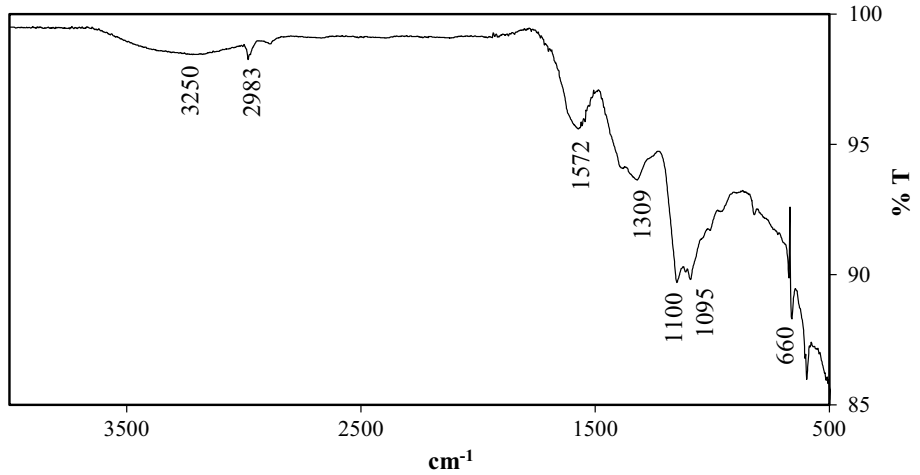

Fig. 3 FT-IR spectrum of AgNPs

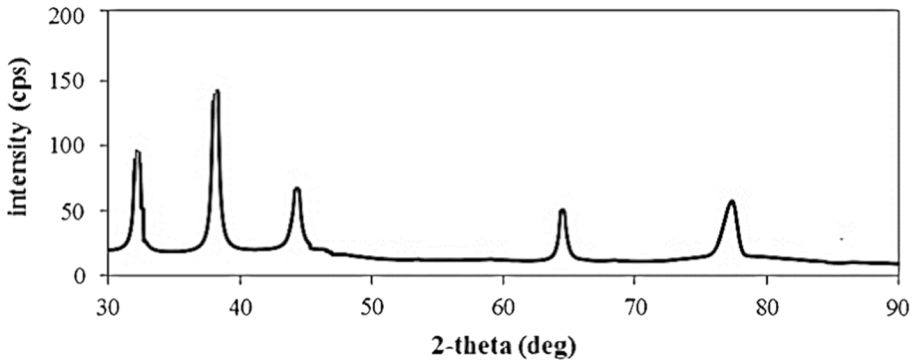

Fig. 4 XRD pattern of AgNPs

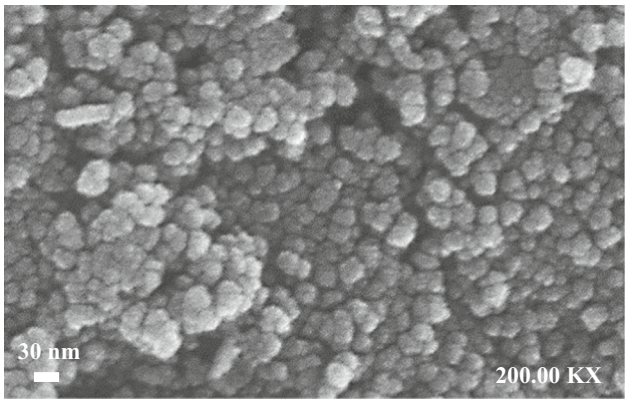

Fig. 5 SEM image of AgNPs

The size distribution analysis of AgNPs was performed by DLS analysis method, and the observed results are shown in Fig. 6. Accordingly, the average hydraulic diameter of AgNPs was found to be 22.07 nm with a low polydispersity index of 0.238.

3.1.1 The Mechanism of Nanoparticle Formation

The formation of AgNPs in both of chemical synthesis and biosynthesis methods depends on the reduction of Ag^{1+} ions to Ag^0 with the reductant agent, which is $NaBH_4$ in the chemical synthesis, phenolic compounds in the biosynthesis. The proposed mechanisms for the chemical synthesis and the biosynthesis were given in Eqs. (1) and (2), respectively [44].

$$2AgNO_3 + 2NaBH_{4(\text{as reductant agent})} \rightarrow 2Ag^0 + H_2 + B_2H_6 + 2NaNO_3 \quad (1)$$

$$AgNO_3 + \text{phenolic compounds}_{(\text{as reductant agent})} \rightarrow Ag^0 + \text{byproducts} \quad (2)$$

The yields of these reactions were calculated with the following equation:

$$Y\% = \frac{m_{AgNPs}}{m_{AgNO_3}} \times 100 \quad (3)$$

By using Eq. (3), the yields of the chemical synthesis and the biosynthesis reactions were calculated to be 95.24% and 94.23%, respectively. The yield of the chemical synthesis reaction was slightly higher than that of the biosynthesis reaction, indicating that the biosynthesis method with as high yield as the chemical synthesis could be efficiently used for the synthesis of AgNPs.

3.2 Colorimetric Detection of Metal Ions with AgNPs

In this study, the colorimetric detection of the metal ions with AgNPs synthesized from *B. variegata* leaf extract was investigated. Firstly, the selectivity of the biosynthesized AgNPs as a colorimetric sensor for various metal ions (Na^+, K^+, Mg^{2+}, Ba^{2+}, Ni^{2+}, Mn^{2+}, Cu^{2+}, Zn^{2+}, Cd^{2+}, and Fe^{3+}) has been evaluated. For this purpose, uniform concentration of various metal salt solutions (1000 µM) was separately added to the biosynthesized AgNPs solutions; after that, the color changes of the prepared solutions were firstly observed visually, and then, the absorption spectra were recorded for AgNPs solutions in the absence and presence of various metal ions. The photographs and UV–Vis spectra of AgNPs solutions and also the bar chart plotted by using differences between the absorbance of AgNPs solution in the absence and presence of various metal ions are presented in Fig. 7a–c, respectively.

It was clearly seen from Fig. 7a, b that AgNPs solution containing only Fe^{3+} ions had the color change from brown to colorless and also λ_{SPR} of AgNPs solution containing only Fe^{3+} ions disappeared, while the colors and λ_{SPR} intensities of AgNPs solutions showed very slight or even no significant changes in the presence of Na^+, K^+, Mg^{2+}, Ba^{2+}, Ni^{2+}, Mn^{2+}, Cu^{2+}, Zn^{2+}, and Cd^{2+} ions.

Furthermore, as shown in Fig. 7c, the bar of AgNPs solution in the presence of Fe^{3+} was much higher than the other metal cations, which stated that other metal cations except

(a)

Size d.nm	Mean Number %	Std Dev Number %	Size d.nm	Mean Number %	Std Dev Number %	Size d.nm	Mean Number %	Std Dev Number %	Size d.nm	Mean Number %	Std Dev Number %
0,4000	0,0		5,615	0,0		78,82	0,0		1106	0,0	
0,4632	0,0		6,503	0,0		91,28	0,0		1281	0,0	
0,5365	0,0		7,531	0,0		105,7	0,0		1484	0,0	
0,6213	0,0		8,721	0,0		122,4	0,0		1718	0,0	
0,7195	0,0		10,10	0,0		141,8	0,0		1990	0,0	
0,8332	0,0		11,70	0,0		164,2	0,0		2305	0,0	
0,9649	0,0		13,54	0,0		190,1	0,0		2669	0,0	
1,117	0,0		15,69	5,0		220,2	0,0		3091	0,0	
1,294	0,0		18,17	18,3		255,0	0,0		3580	0,0	
1,499	0,0		21,04	27,8		295,3	0,0		4145	0,0	
1,736	0,0		24,36	24,2		342,0	0,0		4801	0,0	
2,010	0,0		28,21	14,4		396,1	0,0		5560	0,0	
2,328	0,0		32,67	6,5		458,7	0,0		6439	0,0	
2,696	0,0		37,84	2,4		531,2	0,0		7456	0,0	
3,122	0,0		43,82	0,8		615,1	0,0		8635	0,0	
3,615	0,0		50,75	0,3		712,4	0,0		1,000e4	0,0	
4,187	0,0		58,77	0,1		825,0	0,0				
4,849	0,0		68,06	0,1		955,4	0,0				

(b)

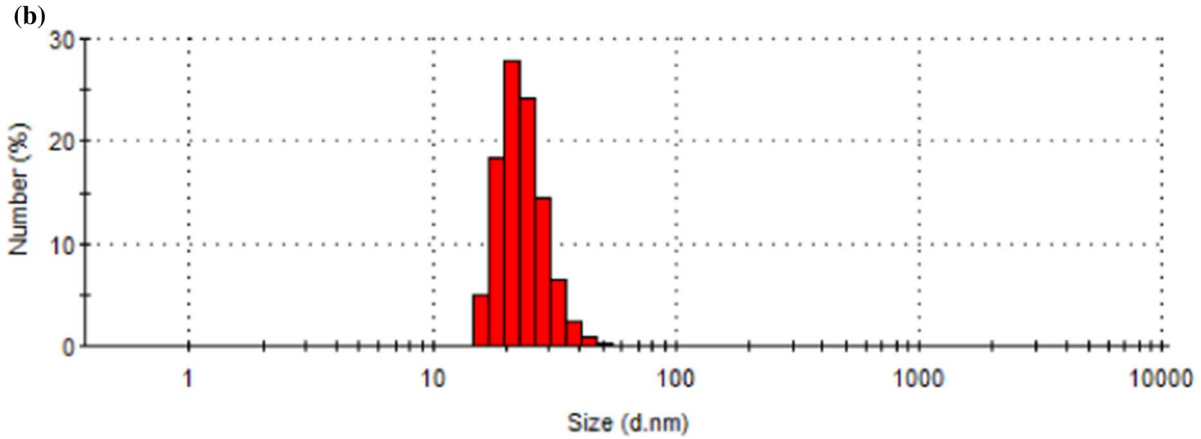

Fig. 6 Size distribution results of AgNPs

Fe^{3+} ions had little influence on the biosynthesized AgNPs. The obtained results clearly showed that the biosynthesized AgNPs colorimetric sensor has a good selectivity toward the sensing of Fe^{3+} ions over other cations.

In order to determine the sensitivity of the biosynthesized AgNPs colorimetric sensor for Fe^{3+} sensing, the changes in the AgNPs solution color and λ_{SPR} intensity for different concentrations of Fe^{3+} were evaluated, and the obtained results are presented in Fig. 8a, b. It was evident that as the concentration of Fe^{3+} increased from 1.0 µM to 1000 µM, the color of AgNPs solution altered progressively from brown to colorless (Fig. 8a), and also, λ_{SPR} intensities of AgNPs solutions containing Fe^{3+} ions at different concentrations decreased gradually (Fig. 8b). These results suggested that the biosynthesized AgNPs exhibited Fe^{3+} concentration-dependent colorimetric response.

The limit of detection for Fe^{3+} ions of the biosynthesized AgNPs colorimetric sensor was determined from three times the standard deviation of the blank signal (LOD = 3σ/s). Figure 9 infers that Fe^{3+} concentration-dependent colorimetric responses of AgNPs were linearly proportional to the concentration of Fe^{3+} ions between 6.0 and 100 µM, and also, LOD for Fe^{3+} ions of AgNPs colorimetric sensor was determined to be 2.08×10^{-6} M. A literature survey was carried out for the colorimetric detection of Fe^{3+} ions with AgNPs, and it was concluded that there have been a limited number of studies about it. Among the existing studies about the detection of Fe^{3+} ions by AgNPs, Bothra et al. [51] determined the LOD of p-PDA functionalized AgNPs as 1.29×10^{-6} M and Zhan et al. [24] calculated the LOD of pyridyl-appended calix [4] arene functionalized AgNPs as 1.25×10^{-4} M. As seen in the studies in the literature, the functionalized AgNPs have been generally used for the colorimetric detection of Fe^{3+} ions. Consequently, the obtained detection limit of the biosynthesized AgNPs in this study was quite competitive with the reported AgNPs colorimetric sensor, indicating efficient usability for the colorimetric detection of Fe^{3+} ions.

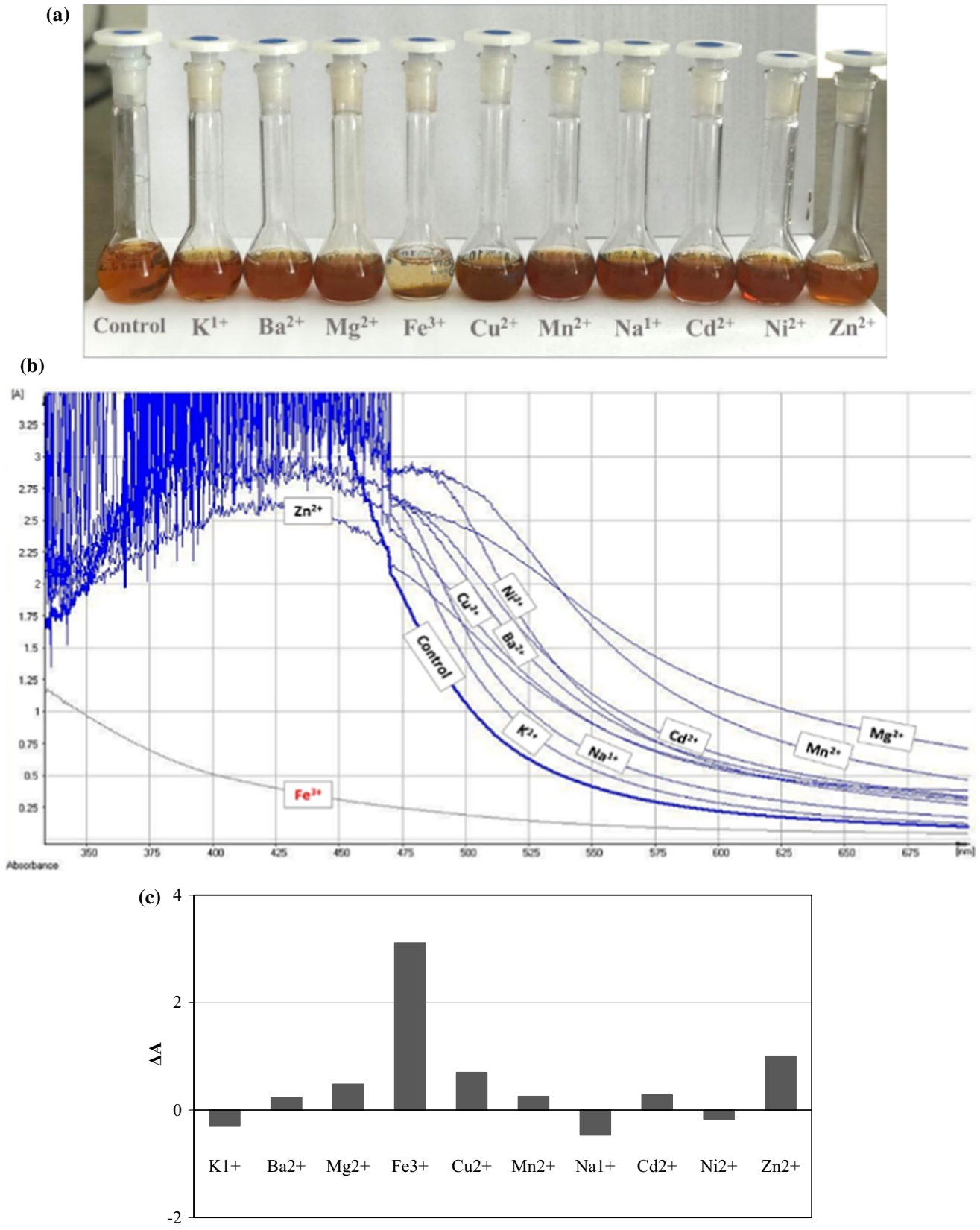

Fig. 7 **a** The photographs of AgNPs solutions in the absence and presence of various metal ions. **b** UV–Vis spectra of AgNPs solutions in the absence and presence of various metal ions. **c** The changes in λ_{SPR} values of AgNPs solution containing various metal ions ($\Delta A = A_o - A$)

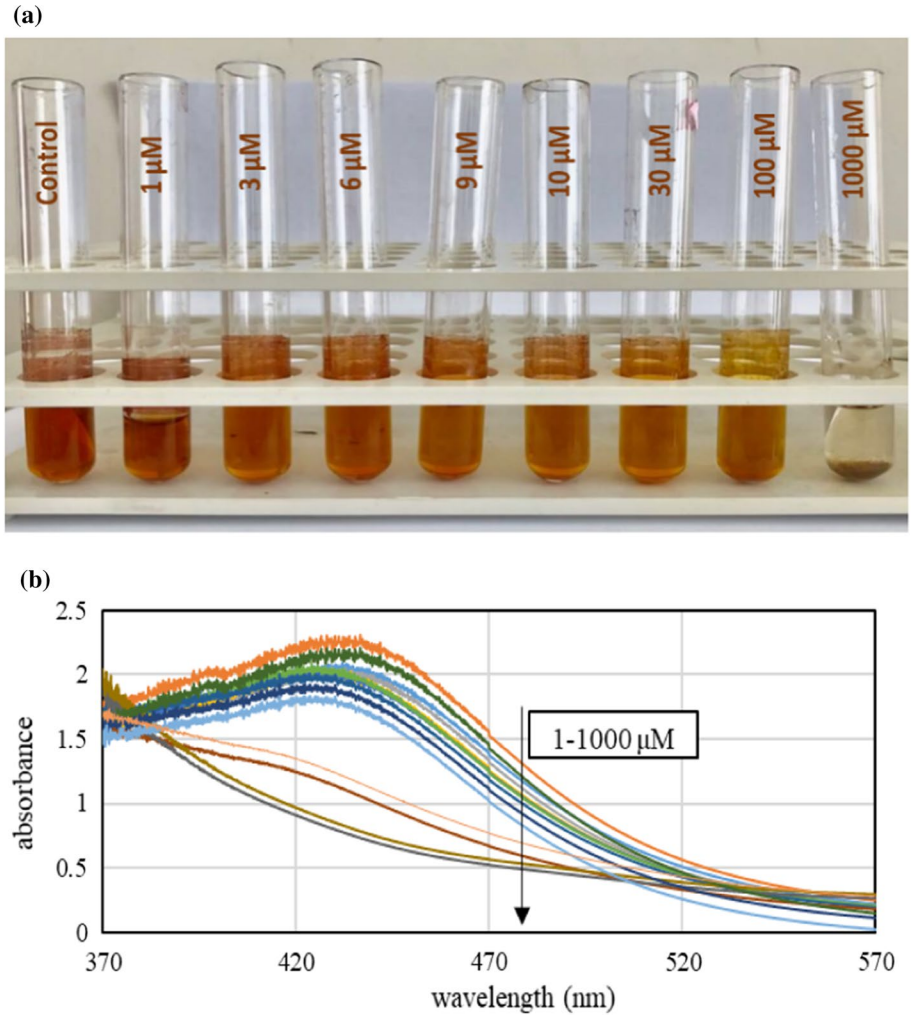

Fig. 8 **a** The photographs of AgNPs solutions in the absence and presence of Fe^{3+} ions at different concentrations. **b** UV–Vis spectra of AgNPs solutions in the absence and presence of Fe^{3+} ions at different concentrations

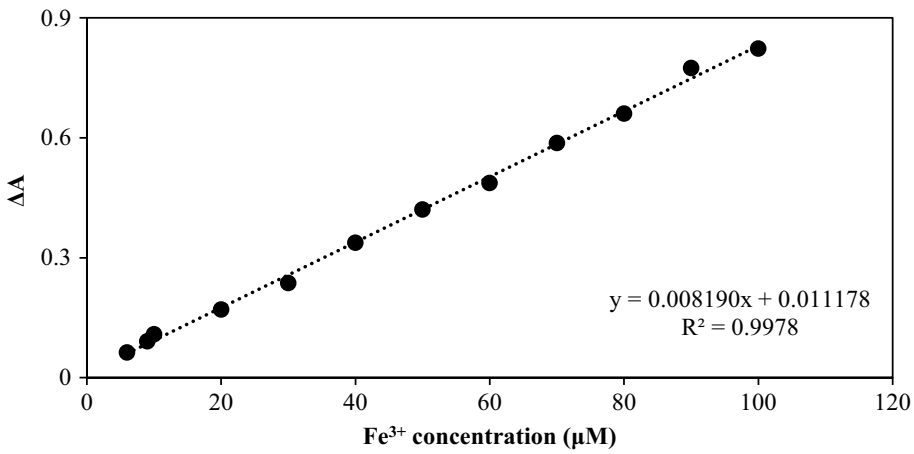

Fig. 9 The plot of ΔA values for biosynthesized AgNPs solutions containing Fe^{3+} ions at different concentrations vs Fe^{3+} concentration

For the comparison of chemically synthesized AgNPs with biosynthesized AgNPs, AgNPs were synthesized via chemical reduction method. After confirmed the formation of AgNPs with UV–Vis spectrum scan, the studies of colorimetric detection of Fe^{3+} with chemically synthesized AgNPs were carried out. For this purpose, 1.0 mL of different concentrations of Fe^{3+} ion (1.0–100 µM) solutions was added to the mixture containing 2.0 mL of 0.15 g/L AgNPs solution and 1.0 mL of the distilled water. Approximately 5.0 min later, the absorbance value of the prepared solution

was recorded at 400 nm by UV–Vis spectrophotometer. By using the decreasing in the λ_{SPR} intensity of AgNPs with the addition of Fe^{3+} ion solutions at different concentrations, the linear detectable range and the limit of detection (LOD = 3σ/s) were determined. Figure 10 shows the linear relationship between the SPR peak intensity difference and the concentration of Fe^{3+} within the range from 30 to 100 µM. The fitting line can be expressed as $\Delta A = 0.0006899\,[Fe^{3+}] - 0.01335$ with a linear regression coefficient (R^2) of 0.9972. Under the current experimental conditions, the LOD value was calculated to be 2.47×10^{-5} M on the basis of a signal to noise of 3 (LOD = 3σ/s). When compared this LOD value with the biosynthesized AgNPs in this study (LOD = 2.08×10^{-6} M), it could be clearly seen that the LOD value was higher and the linear detectable range was narrower, designating inefficient usability of the chemically synthesized AgNPs for the colorimetric detection of Fe^{3+} ions. This case indicated that the chemically synthesized AgNPs could not compete with the biosynthesized AgNPs in this study and the other sensors in the literature.

The detection mechanism principle of Fe^{3+} ions by the biosynthesized AgNPs is based on the reduction–oxidation reaction. Table 1 exhibits standard reduction potentials for several elements [52].

Theoretically, it is known that the redox reaction that has positive cell potential (E^{o}_{cell} value) occurs spontaneously. For example, according to Eqs. (4)–(6); redox reactions of Ag-Cr^{3+} and Ag-Na^{1+} that have negative E^{o}_{cell} values do not take place, while the spontaneous redox reaction between Ag-Hg^{2+} can take place due to the positive E^{o}_{cell} value [53]. However, as shown in Table 1, the potentials of Fe^{3+}/Fe^{2+} (+0.77 V) and Fe^{3+}/Fe (−0.04 V) are lower than the potential of Ag^{1+}/Ag (+0.80 V). Due to the negative E^{o}_{cell} values (for [Fe^{3+}/Fe^{2+}]–Ag $E^{o}_{cell} = 0.77–0.80 = -0.03$ V; for [Fe^{3+}/Fe]–Ag $E^{o}_{cell} = -0.04$ to $0.80 = -0.84$ V), ferric ions do not have enough ability to oxidize elemental silver (AgNPs). This case could be explained with the presence of halide ions (Cl^- ions arising from $FeCl_3$ metal salt solution) in the detection media. The halide ions could strongly coordinate with silver species, resulting in a significant decrease in the reduction potential of the silver species. On the other hand, although the halide ions also have similar influences on iron species, it causes a much smaller decrease in the potential of Fe^{3+}/Fe^{2+} than the case of silver species. The much higher decrease in the potential of Ag^{1+}/Ag enables the oxidation of elemental silver by ferric ions to become possible by providing positive E^{o}_{cell} value. Thus, the redox reaction between AgNPs and Fe^{3+} ions [$Ag + Fe^{3+} \rightarrow Ag^{1+} + Fe^{2+}$] occurs spontaneously [18, 54, 55].

$$2Ag + 2Hg^{2+} \rightarrow 2Ag^{1+} + Hg_2^{2+} \quad E^{o}_{cell} = +0.12\ V \tag{4}$$

$$3Ag + Cr^{3+} \rightarrow 3Ag^{+} + Cr \quad E^{o}_{cell} = -1.54\ V \tag{5}$$

$$Ag + Na^{1+} \rightarrow Ag^{1+} + Na \quad E^{o}_{cell} = -3.51\ V \tag{6}$$

The schematic display of the predicted redox reaction, as well as the colorimetric detection of Fe^{3+} ions by the biosynthesized AgNPs, is presented in Fig. 11. Accordingly; as a result of redox reaction between Fe^{3+} ions and the biosynthesized AgNPs, the color of AgNPs solution decolorized

Table 1 Standard reduction potentials at 298 K

Reduction reaction	E° (V)	Reduction reaction	E° (V)
$Au^{1+} + e^- \Rightarrow Au$	+1.69	$Co^{2+} + 2e^- \Rightarrow Co$	−0.28
$Au^{3+} + 3e^- \Rightarrow Au$	+1.40	$Fe^{2+} + 2e^- \Rightarrow Fe$	−0.44
$2Hg^{2+} + 2e^- \Rightarrow Hg_2^{2+}$	+0.92	$Cr^{3+} + 3e^- \Rightarrow Cr$	−0.74
$Hg^{2+} + 2e^- \Rightarrow Hg$	+0.86	$Zn^{2+} + 2e^- \Rightarrow Zn$	−0.76
$Ag^{1+} + e^- \Rightarrow Ag$	+0.80	$Mn^{2+} + 2e^- \Rightarrow Mn$	−1.18
$Hg_2^{2+} + 2e^- \Rightarrow 2Hg$	+0.79	$Al^{3+} + 3e^- \Rightarrow Al$	−1.66
$Fe^{3+} + e^- \Rightarrow Fe^{2+}$	+0.77	$Ca^{2+} + 2e^- \Rightarrow Ca$	−2.87
$Fe^{3+} + 3e^- \Rightarrow Fe$	−0.04	$Na^{1+} + e^- \Rightarrow Na$	−2.71

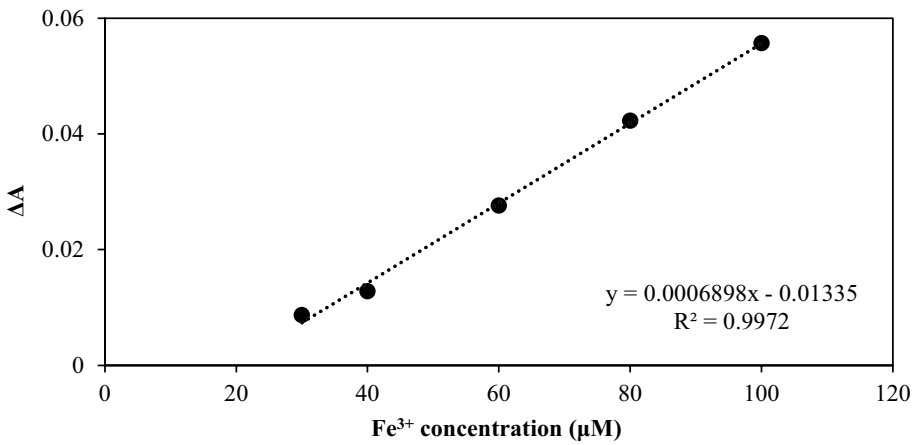

Fig. 10 The plot of ΔA values for the chemically synthesized AgNPs solutions containing Fe^{3+} ions at different concentrations vs Fe^{3+} concentration

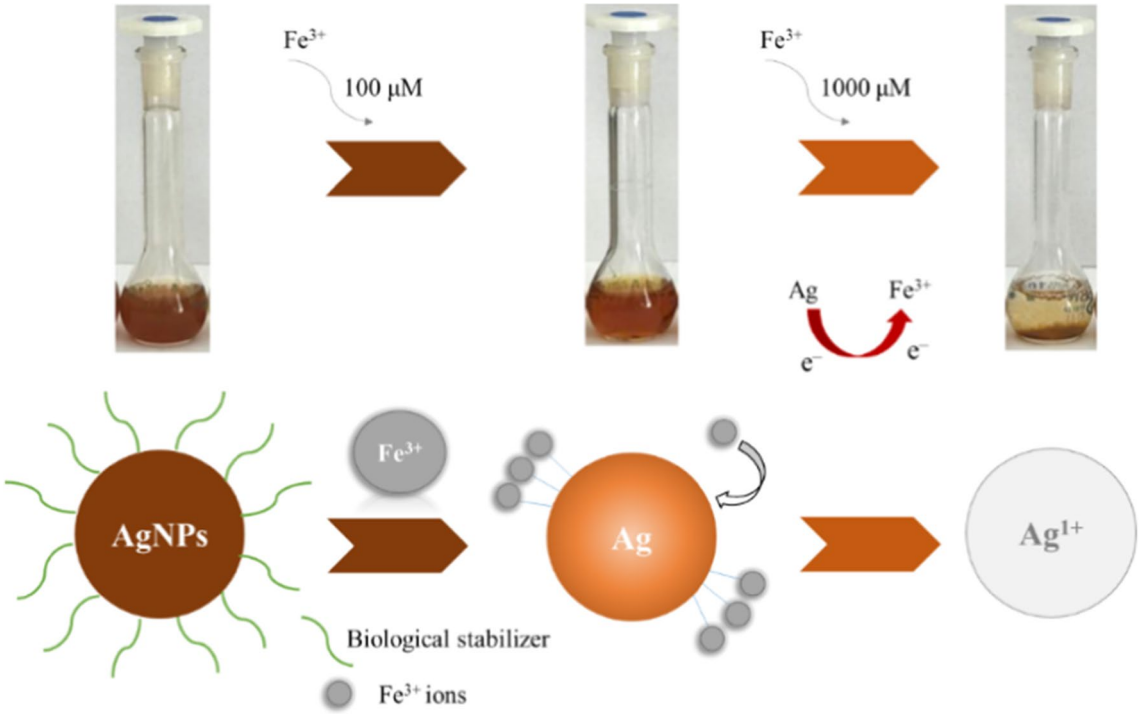

Fig. 11 The illustration of the detection of Fe^{3+} ions by the biosynthesized AgNPs

relatively by adding of Fe^{3+} ions at 100 µM, while the color vanished by adding of Fe^{3+} ions at 1000 µM.

4 Conclusion

In the present study, AgNPs could be synthesized successfully by using orchid tree (*B. variegata*) leaf extract as an eco-friendly, non-toxic, and cost-effective reducing agent. By this way, the evaluating of *B. variegata* leaves in metallic nanoparticle biosynthesis provides to convert an unused agricultural waste into economic value. Then, the biosynthesized AgNPs were evaluated as a colorimetric sensor. The biosynthesized AgNPs had selectivity to only Fe^{3+} ions. The limit of detection for Fe^{3+} ions of AgNPs colorimetric sensor was determined to be 2.08×10^{-6} M, which is relatively better compared to the related literature. Moreover, the detection limits of studies about the detection of metal ions by ordinary spectrophotometric methods in the literature are not too lower than this study; they are quite close to the detection limit of this study. Therefore, it can be concluded that the biosynthesized AgNPs in this study have the potential to compete with them especially cost-wise. Consequently, the obtained results showed that the biosynthesized AgNPs could be used as an effective colorimetric sensor for the detection of Fe^{3+} ions in aqueous solution. On the other hand, the present work has revealed significant outputs to the synthesis of an eco-friendly and non-functionalized colorimetric sensor, which could be important for the contribution to the related literature as well as the colorimetric detection applications.

References

1. Carolin, C.F.; Kumar, P.S.; Saravanan, A.; Joshiba, G.J.; Naushad, M.: Efficient techniques for the removal of toxic heavy metals from aquatic environment: a review. J. Environ. Chem. Eng. **5**(3), 2782–2799 (2017)
2. Tüzen, M.: Determination of heavy metals in fish samples of the middle Black Sea (Turkey) by graphite furnace atomic absorption spectrometry. Food Chem. **80**(1), 119–123 (2003)
3. Aydin, F.A.; Soylak, M.: Separation, preconcentration and inductively coupled plasma-mass spectrometric (ICP-MS) determination of thorium (IV), titanium (IV), iron (III), lead (II) and chromium (III) on 2-nitroso-1-naphthol impregnated MCI GEL CHP20P resin. J. Hazard. Mater. **173**(1–3), 669–674 (2010)
4. Donohue, S.J.; Aho, D.W.; Plank, C.O.: Determination of P, K, Ca, Mg, Mn, Fe, Al, B, Cu, and Zn in plant tissue by inductively coupled plasma (ICP) emission spectroscopy. Plant Anal. Ref. Proced. South. Reg. US **7**, 34–37 (1992)
5. Şenyuva, H.Z.; Sarica, D.Y.; Özden, T.: Simultaneous determination of Fe(II) and Fe(III) in pharmaceutical samples by post-column derivatization/HPLC. Turk. J. Chem. **26**(3), 425–430 (2002)
6. Gholivand, M.B.; Geravandi, B.; Parvin, M.H.: Anodic stripping voltammetric determination of iron (II) at a carbon paste electrode modified with dithiodianiline (DTDA) and gold nanoparticles (GNP). Electroanal. **23**(6), 1345–1351 (2011)
7. Segura, R.; Toral, M.I.; Arancibia, V.: Determination of iron in water samples by adsorptive stripping voltammetry with a bismuth

film electrode in the presence of 1-(2-piridylazo)-2-naphthol. Talanta **75**(4), 973–977 (2008)
8. Yaqoob, M.; Waseem, A.; Nabi, A.: Determination of total iron in fresh waters using flow injection with potassium permanganate chemiluminescence detection. J. Anal. Chem. **61**(9), 917–921 (2006)
9. Guzar, S.H.; Jin, Q.H.: Simple, selective, and sensitive spectrophotometric method for determination of trace amounts of nickel (II), copper (II), cobalt (II), and iron (III) with a novel reagent 2-pyridine carboxaldehyde isonicotinyl hydrazone. Chem. Res. Chin. Univ. **24**(2), 143–147 (2008)
10. Annadhasan, M.; Kasthuri, J.; Rajendiran, N.: A facile sunlight-induced synthesis of phenylalanine-conjugated cholic acid-stabilized silver and gold nanoparticles for colorimetric detection of toxic Hg2 + , Cr6 + and Pb2 + ions. Chem. Sel. **4**(21), 6557–6567 (2019)
11. Giokas, D.L.; Paleologos, E.K.; Karayannis, M.I.: Speciation of Fe(II) and Fe(III) by the modified ferrozine method, FIA–spectrophotometry, and flame AAS after cloud-point extraction. Anal. Bioanal. Chem. **373**(4–5), 237–243 (2002)
12. Blain, S.; Treguer, P.: Iron (II) and iron (III) determination in sea water at the nanomolar level with selective on-line preconcentration and spectrophotometric determination. Anal. Chim. **308**(1–3), 425–432 (1995)
13. Liang, Z.Q.; Wang, C.X.; Yang, J.X.; Gao, H.W.; Tian, Y.P.; Tao, X.T.; Jiang, M.H.: A highly selective colorimetric chemosensor for detecting the respective amounts of iron (II) and iron (III) ions in water. New J. Chem. **31**(6), 906–910 (2007)
14. Kass, M.; Ivaska, A.: Spectrophotometric determination of iron (III) and total iron by sequential injection analysis technique. Talanta **58**(6), 1131–1137 (2002)
15. Mulaudzi, L.V.; van Staden, J.F.; Stefan, R.I.: On-line determination of iron (II) and iron (III) using a spectrophotometric sequential injection system. Anal. Chim. **467**(1–2), 35–49 (2002)
16. Ohno, S.; Teshima, N.; Sakai, T.; Grudpan, K.; Polasek, M.: Sequential injection lab-on-valve simultaneous spectrophotometric determination of trace amounts of copper and iron. Talanta **68**(3), 527–534 (2006)
17. Abdollahi, H.: Simultaneous spectrophotometric determination of chromium (VI) and iron (III) with chromogenic mixed reagents by H-point standard addition method and partial least squares regression. Anal. Chim. **442**(2), 327–336 (2001)
18. Gao, X.; Lu, Y.; He, S.; Li, X.; Chen, W.: Colorimetric detection of iron ions (III) based on the highly sensitive plasmonic response of the N-acetyl-L-cysteine-stabilized silver nanoparticles. Anal. Chim. Acta **879**, 118–125 (2015)
19. Qu, K.; Wang, J.; Ren, J.; Qu, X.: Carbon dots prepared by hydrothermal treatment of dopamine as an effective fluorescent sensing platform for the label-free detection of iron (III) ions and dopamine. Chem. Eur. J. **19**(22), 7243–7249 (2013)
20. Tripathy, S.K.; Woo, J.Y.; Han, C.S.: Colorimetric detection of Fe(III) ions using label-free gold nanoparticles and acidic thiourea mixture. Sens. Actuators B Chem. **181**, 114–118 (2013)
21. Salimi, F.; Kiani, M.; Karami, C.; Taher, M.A.: Colorimetric sensor of detection of Cr(III) and Fe(II) ions in aqueous solutions using gold nanoparticles modified with methylene blue. Optik **158**, 813–825 (2018)
22. Wu, S.P.; Chen, Y.P.; Sung, Y.M.: Colorimetric detection of Fe^{3+} ions using pyrophosphate functionalized gold nanoparticles. Analyst **136**(9), 1887–1891 (2011)
23. Bothra, S.; Solanki, J.N.; Sahoo, S.K.: Functionalized silver nanoparticles as chemosensor for pH, Hg^{2+} and Fe^{3+} in aqueous medium. Sens. Actuators B-Chem. **188**, 937–943 (2013)
24. Zhan, J.; Wen, L.; Miao, F.; Tian, D.; Zhu, X.; Li, H.: Synthesis of a pyridyl-appended calix [4] arene and its application to the modification of silver nanoparticles as an Fe^{3+} colorimetric sensor. New J. Chem. **36**(3), 656–661 (2012)
25. Buduru, P.: Oxamic acid and p-aminobenzoic acid functionalized gold nanoparticles as a probe for colorimetric detection of Fe^{3+} ion. Sens. Actuators B Chem. **237**, 935–943 (2016)
26. Sabour, B.; Kheirifam, M.: Electrochemical synthesis of magnetite nanoparticles and their doping with Cu^{2+} cations and surface coating with polyethylenimine. Anal. Bioanal. Electrochem. **11**(1), 99–107 (2019)
27. Lapp, A.S.; Duan, Z.; Marcella, N.; Luo, L.; Genc, A.; Ringnalda, J.; Crooks, R.M.: Experimental and theoretical structural investigation of AuPt nanoparticles synthesized using a direct electrochemical method. J. Am. Chem. Soc. **140**(20), 6249–6259 (2018)
28. Lone, I.H.; Ahmed, J.; Ahmad, T.: Reverse micellar synthesis, characterization, magnetic and ferroelectric properties of $YFeO_3$ nanoparticles. Mater. Today Proc. **5**(7), 15303–15310 (2018)
29. Tianimoghadam, S.; Salabat, A.: A microemulsion method for preparation of thiol-functionalized gold nanoparticles. Particuology **37**, 33–36 (2018)
30. Safaei, M.; Beitollahi, H.; Shishehbore, M.R.: Synthesis and characterization of $NiFe_2O_4$ nanoparticles using the hydrothermal method as magnetic catalysts for electrochemical detection of norepinephrine in the presence of folic acid. J. Chin. Chem. Soc. (2019). https://doi.org/10.1002/jccs.201900073
31. Zhang, X.; Sun, H.; Tan, S.; Gao, J.; Fu, Y.; Liu, Z.: Hydrothermal synthesis of Ag nanoparticles on the nanocellulose and their antibacterial study. Inorg. Chem. Commun. **100**, 44–50 (2019)
32. Yusof, N.S.M.; Ashokkumar, M.: Sonochemical synthesis of gold nanoparticles by using high intensity focused ultrasound. Chem. Phys. Chem. **16**(4), 775–781 (2015)
33. Vinoth, V.; Wu, J.J.; Asiri, A.M.; Anandan, S.: Sonochemical synthesis of silver nanoparticles anchored reduced graphene oxide nanosheets for selective and sensitive detection of glutathione. Ultrason. Sonochem. **39**, 363–373 (2017)
34. Ghorbani, H.R.; Mehr, F.P.; Pazoki, H.; Rahmani, B.M.: Synthesis of ZnO nanoparticles by precipitation method. Orient. J. Chem. **31**(2), 1219–1221 (2015)
35. Lassoued, A.; Dkhil, B.; Gadri, A.; Ammar, S.: Control of the shape and size of iron oxide (α-Fe_2O_3) nanoparticles synthesized through the chemical precipitation method. Res. Phys. **7**, 3007–3015 (2017)
36. Guzmán, M.G.; Dille, J.; Godet, S.: Synthesis of silver nanoparticles by chemical reduction method and their antibacterial activity. Int. J. Chem. Biomol. Eng. **2**(3), 104–111 (2009)
37. Sugimoto, T.; Zhou, X.; Muramatsu, A.: Synthesis of uniform anatase TiO_2 nanoparticles by gel–sol method: 4. Shape Control. J. Colloid Interf. Sci. **259**(1), 53–61 (2003)
38. Veerasamy, R.; Xin, T.Z.; Gunasagaran, S.; Xiang, T.F.W.; Yang, E.F.C.; Jeyakumar, N.; Dhanaraj, S.A.: Biosynthesis of silver nanoparticles using mangosteen leaf extract and evaluation of their antimicrobial activities. J. Saudi Chem. Soc. **15**(2), 113–120 (2011)
39. Kalaiselvi, D.; Mohankumar, A.; Shanmugam, G.; Nivitha, S.; Sundararaj, P.: Green synthesis of silver nanoparticles using latex extract of Euphorbia tirucalli: a novel approach for the management of root knot nematode, Meloidogyne incognita. Crop Prot. **117**, 108–114 (2019)
40. Sithara, R.; Selvakumar, P.; Arun, C.; Anandan, S.; Sivashanmugam, P.: Economical synthesis of silver nanoparticles using leaf extract of Acalypha hispida and its application in the detection of Mn(II) ions. J. Adv. Res. **8**(6), 561–568 (2017)
41. Puente, C.; Gómez, I.; Kharisov, B.; López, I.: Selective colorimetric sensing of Zn(II) ions using green-synthesized silver nanoparticles: ficus benjamina extract as reducing and stabilizing agent. Mater. Res. Bull. **112**, 1–8 (2019)

42. Slinkard, K.; Singleton, V.L.: Total phenol analysis: automation and comparison with manual methods. Am. J. Enol. Vitic. **28**(1), 49–55 (1977)
43. Gade, A.; Gaikwad, S.; Duran, N.; Rai, M.: Green synthesis of silver nanoparticles by Phoma glomerata. Micron **59**, 52–59 (2014)
44. Mulfinger, L.; Solomon, S.D.; Bahadory, M.; Jeyarajasingam, A.V.; Rutkowsky, S.A.; Boritz, C.: Synthesis and study of silver nanoparticles. J. Chem. Educ. **84**(2), 322 (2007)
45. Veisi, H.; Azizi, S.; Mohammadi, P.: Green synthesis of the silver nanoparticles mediated by *Thymbra spicata* extract and its application as a heterogeneous and recyclable nanocatalyst for catalytic reduction of a variety of dyes in water. J. Clean. Prod. **170**, 1536–1543 (2018)
46. Siddiqui, M.N.; Redhwi, H.H.; Achilias, D.S.; Kosmidou, E.; Vakalopoulou, E.; Ioannidou, M.D.: Green synthesis of silver nanoparticles and study of their antimicrobial properties. J. Polym. Environ. **26**(2), 423–433 (2018)
47. Kathiraven, T.; Sundaramanickam, A.; Shanmugam, N.; Balasubramanian, T.: Green synthesis of silver nanoparticles using marine algae Caulerpa racemosa and their antibacterial activity against some human pathogens. Appl. Nanosci. **5**(4), 499–504 (2015)
48. Muthukumaran, U.; Govindarajan, M.; Rajeswary, M.; Hoti, S.L.: Synthesis and characterization of silver nanoparticles using Gmelina asiatica leaf extract against filariasis, dengue, and malaria vector mosquitoes. Parasitol. Res. **114**(5), 1817–1827 (2015)
49. Mishra, P.M.; Sahoo, S.K.; Naik, G.K.; Parida, K.: Biomimetic synthesis, characterization and mechanism of formation of stable silver nanoparticles using *Averrhoa carambola* L. leaf extract. Mater. Lett. **160**, 566–571 (2015)
50. Sathyavathi, R.; Krishna, M.B.; Rao, S.V.; Saritha, R.; Rao, D.N.: Biosynthesis of silver nanoparticles using *Coriandrum sativum* leaf extract and their application in nonlinear optics. Adv. Sci. Lett. **3**(2), 138–143 (2010)
51. Bothra, S.; Solanki, J.N.; Sahoo, S.K.: Functionalized silver nanoparticles as chemosensor for pH, Hg^{2+} and Fe^{3+} in aqueous medium. Sens. Actuators B Chem. **188**, 937–943 (2013)
52. Firdaus, M.L.; Fitriani, I.; Wyantuti, S.; Hartati, Y.W.; Khaydarov, R.; McAlister, J.A.; Gamo, T.: Colorimetric detection of mercury (II) ion in aqueous solution using silver nanoparticles. Anal. Sci. **33**(7), 831–837 (2017)
53. Firdaus, M.; Andriana, S.; Alwi, W.; Swistoro, E.; Ruyani, A.; Sundaryono, A.: Green synthesis of silver nanoparticles using Carica Papaya fruit extract under sunlight irradiation and their colorimetric detection of mercury ions. J. Phys. Conf. Ser. **817**(1), 1–6 (2017)
54. Zou, R.; Guo, X.; Yang, J.; Li, D.; Peng, F.; Zhang, L.; Yu, H.: Selective etching of gold nanorods by ferric chloride at room temperature. Cryst. Eng. Commun. **11**(12), 2797–2803 (2009)
55. Liu, J.M.; Jiao, L.; Cui, M.L.; Lin, L.P.; Wang, X.X.; Zheng, Z.Y.; Jiang, S.L.: A highly sensitive non-aggregation colorimetric sensor for the determination of I − based on its catalytic effect on Fe^{3+} etching gold nanorods. Sens. Actuators B Chem. **188**, 644–650 (2013)